Laminin Induces the Stable Expression of Surface Galactosyltransferase on Lamellipodia of Migrating Cells

David J. Eckstein and Barry D. Shur

Department of Biochemistry and Molecular Biology, University of Texas, M. D. Anderson Cancer Center, Houston, Texas 77030

Abstract. We have previously shown that cell surface galactosyltransferase (GalTase) mediates cell spreading and migration on basal lamina matrices by binding N-linked oligosaccharide substrates within laminin. In this study we have examined the distribution and expression of cell surface GalTase during mesenchymal cell migration on various extracellular matrices. Antisera raised against affinity-purified β1,4 GalTase, as well as anti-GalTase Fab fragments, inhibited cell migration on laminin-containing matrices, whereas under identical conditions, anti-GalTase IgG had no effect on the rate of cell migration on fibronectin substrates. Cells migrating on laminin had three times the level of surface GalTase, assayed by ^{125}I-antibody binding and by direct enzyme assay, than similar cells migrating on fibronectin. On the other hand, total cellular GalTase, assayed either enzymatically or by Northern blot analysis, was similar when cells were grown on laminin or fibronectin. The laminin-dependent increase in surface GalTase was due to its expression onto the leading and trailing edges of migrating cells in association with actin-containing microfilaments assayed by double-label indirect immunofluorescence. On stationary cells, surface GalTase levels were low, but as cells began to migrate on laminin GalTase became polarized to the growing lamellipodia. GalTase was not detectable on lamellipodia or filopodia when cells migrated on fibronectin substrates. These results show that laminin-containing matrices induce the stable expression of GalTase onto cell lamellipodia and filopodia where it mediates subsequent cell spreading and migration. Since fibronectin was unable to induce GalTase expression onto lamellipodia, these studies also suggest that the extracellular matrix can selectively influence which intracellular components are maintained on the cell surface.

TEMPORALLY and spatially specific cell migrations are of obvious importance during embryonic morphogenesis and metastasis (14). Cells are thought to migrate in response to signals within the basal lamina and extracellular matrix (20). A variety of extracellular components have been identified along the paths of cell migration in situ that support cell migration in vitro, including fibronectin, laminin, proteoglycans, as well as others (19, 21, 27, 28).

Several cell surface receptors have been identified that participate during specific cellular interactions by binding components of the extracellular matrix. The best studied class of receptors, the "integrins," mediate cell attachment to fibronectin and to a lesser extent laminin, as well as to a number of other cell surface and matrix glycoproteins that possess the appropriate peptide-binding domain (7, 26). The integrins, however, are just one of many cell surface receptors that recognize specific extracellular components, and it is not yet clear how different surface receptors function collectively to mediate diverse aspects of cell–matrix interactions (1, 4, 7–10, 13, 22, 26, 29, 39, 41).

One recently identified laminin receptor is the cell surface enzyme β1,4 galactosyltransferase (GalTase),[1] which participates during cell migration on basal lamina matrices by binding to specific N-linked oligosaccharide substrates within laminin (28, 29). Like the integrins, GalTase is found on several cell types and has been shown to function during a variety of cellular interactions (2, 12, 16, 24, 25, 28, 30, 32, 33, 35, 40). The level of surface GalTase activity is regulated by mutations of the murine *T/t* complex which influence, directly or indirectly, a variety of cellular interactions during fertilization and development (34, 36). For example, *T/T* embryos are characterized by defective mesenchymal cell migration and a coincident four- to sixfold increase in mesenchymal cell surface GalTase activity, suggesting that surface GalTase may participate during cell migration (34). In this regard, reagents that inhibit surface GalTase activity inhibit avian neural crest cell migration on laminin-containing matrices, whereas reagents that stimulate the catalytic turnover of GalTase increase the rate of cell migration (28). However, these studies were limited because of the lack of an appropriate antibody that could be used to probe GalTase function and expression in cell migration more directly.

In this study, we used an anti-GalTase IgG that recognizes murine GalTase (2, 16, 29, 30, 37) to examine the function, distribution, and expression of surface GalTase during cell migration. Anti-GalTase IgG as well as its Fab fragments inhibited cell migration on laminin matrices, but under similar

1. *Abbreviations used in this paper*: GalTase, galactosyltransferase; α-LA, α-lactalbumin; PYS, parietal yolk sac.

conditions had no effect on migration on fibronectin substrates. The GalTase substrate modifier protein, α-lactalbumin (α-LA), similarly inhibited cell migration. The level of surface GalTase was elevated threefold on laminin matrices, which was due to the specific expression and/or stabilization of GalTase on cell lamellipodia and filopodia in association with actin-containing microfilaments. On the other hand, GalTase was not detectable on lamellipodia or filopodia when cells were migrating on fibronectin, even though total cellular GalTase (i.e., surface and intracellular) was equal in cells migrating on laminin and fibronectin. These results show that laminin, but not fibronectin, induces the stable expression of GalTase from intracellular pools into developing lamellipodia where it mediates subsequent migration. Furthermore, the differential expression of surface GalTase implies that the matrix influences which preexisting intracellular components are recruited to or retained on the cell surface.

Materials and Methods

Reagents

Anti-GalTase IgG was prepared as described previously (2, 16). Briefly, β1,4 GalTase from bovine milk was purified to apparent homogeneity using α-LA affinity chromatography and preparative SDS-PAGE. Protein bands containing GalTase activity were excised from the gel and used to immunize rabbits. IgG was isolated by protein A–Sepharose (Sigma Chemical Co., St. Louis, MO) affinity chromatography, dialyzed against DME (Gibco Laboratories, Grand Island, NY), lyophilized, and stored at −70°C. The resulting anti-GalTase IgG recognizes GalTase on mouse cells as defined (*a*) by immunoprecipitation of enzyme activity (2, 29, 30, 37); (*b*) by immunoprecipitation of a single ^{35}S-metabolically labeled membrane protein (2); (*c*) by inhibition of enzyme activity (2, 16); and (*d*) by indirect immunofluorescence (2, 16, 30, 31). Fab fragments were prepared from anti-GalTase IgG using immobilized papain as described by the manufacturer (Pierce Chemical Co., Rockford, IL) and isolated by protein A–Sepharose affinity chromatography. The resulting Fab fragments were free of contaminating Fc fragments and intact IgG as shown by SDS-PAGE. Preimmune and normal rabbit IgG (Sigma Chemical Co.) were reconstituted directly in DME at the indicated concentrations. α-LA and lysozyme (Sigma Chemical Co.) were dialyzed against water, lyophilized, and reconstituted in DME.

Cells

Mesenchymal Cell Explants. Embryos were obtained from matings between inbred C3H mice. The presence of a vaginal plug was considered day 1 of gestation. On day 10 post-plug (9.5 d gestation), the females were killed by cervical dislocation, the uteri removed, and the embryos separated from the decidua in DME supplemented with penicillin and streptomycin (Gibco Laboratories). The head region was severed from the rest of the body at the level of the first branchial arch using tungsten wires and bisected to expose the large population of head mesenchyme. The resulting head halves were placed medial side down in 15-mm tissue culture wells coated with the appropriate extracellular matrix. The wells were filled with 0.5 ml defined medium (DME supplemented with penicillin, streptomycin, 5 μg/ml insulin, 5 μg/ml transferrin, and 5 ng/ml selenium; Collaborative Research Inc., Lexington, MA) and placed in a 37°C, 5% CO_2 incubator for 2–3 d to allow a sufficient number of cells to migrate away from the explant.

Mouse Embryo Fibroblast Cultures. BALB/c 3T3 cells (American Type Culture Collection, Rockville, MD) were cultured on the indicated extracellular matrix in either complete medium (DME supplemented with 15% heat-inactivated calf serum [HyClone Laboratories, Logan, UT], penicillin, streptomycin, and kanamycin) for GalTase enzyme assays and Northern blot analysis, or in GalTase-free, defined medium (see above) for indirect immunofluorescence and ^{125}I-antibody binding assays. Despite the fact that serum-derived GalTase was heat inactivated in complete medium, we wanted to eliminate any potential cross-reactivity when using anti-GalTase IgG. Cells were harvested with 2 mM EDTA in Ca^{++}/Mg^{++}-free Eagle's balanced salt solution from sparse (<20% confluency) or confluent (>90% confluency) cultures and washed before use.

Matrices. Mesenchymal cell explants and BALB/c 3T3 cells were cultured on either purified laminin isolated from Englebreth Holm Swarm matrix as described (28), bovine plasma fibronectin (Bethesda Research Laboratories, Gaithersburg, MD), or on uncoated tissue culture plastic. Studies in which the cell migration rate was quantitated by time-lapse microphotography were conducted using native basement membrane that had been previously deposited by parietal yolk sac (PYS) endoderm cells, and then been subsequently removed as described (28). However, similar results were also obtained using purified laminin rather than PYS basal lamina, consistent with previous results that have shown that the principal GalTase substrate in native and reconstituted basal lamina matrices is laminin (28, 29).

Migration Assay

The rate of cell migration was quantitated by time-lapse microphotography as previously described (28). Briefly, culture dishes containing 2-d-old mesenchymal cell explants were transferred to the incubator stage of a microscope (IM; Olympus Corporation of America, New Hyde Park, NY) equipped with a camera (OM-2; Olympus Corporation of America) and a control box (M.AC; Olympus Corporation of America) autocontrolled to take photographs every 4.3 min. The temperature was maintained at 37°C by an air curtain (Sage Instruments Div., Cambridge, MA) and the atmosphere was supplemented with CO_2 at a rate sufficient to keep the medium at pH 7.2. A representative population of cells was photographed (Kodak Tech Pan, ASA 50; Eastman Kodak Co., Rochester, NY) for 2 h to generate the basal migration rate for the population (denoted as time 0). The medium was then replaced with fresh medium that had been supplemented with either anti-GalTase IgG, anti-GalTase IgG Fab fragments, α-LA, or control reagents (preimmune IgG or lysozyme, respectively) at the indicated concentration. The same population of cells was then photographed for the desired time. The film was developed and the negatives were projected so that the paths of the cell centers could be traced between frames, thus generating the path of cell migration. Populations of cells with little, if any, cell–cell contact were chosen for analysis. The tracings were digitized on an X-Y digitizing board (Kurta Corp., Phoenix, AZ) and path lengths calculated using VIAS software (Ted Pella Inc., Tustin, CA). The mean migration rate for the population was calculated using VSTAT (Ted Pella Inc.) and the experimental rate of migration compared with the basal rate.

The data are presented as a percentage of the basal rate. Each time point represents the migration rate of the population of cells traced, from the previous time point to the current time point, usually over a 2-h period; however, some rates were analyzed at hourly intervals. The number of cells analyzed in each population is given in the text.

Immunoprecipitation of GalTase Activity

Embryonic mouse heads, obtained as outlined above, were placed in solubilization buffer (30 mM *n*-octylglucoside, 120 mM NaCl, 25 mM Na cacodylate, 0.02% NaN_3, 30 mM *N*-acetylglucosamine, 1% BSA, 10 mM $MnCl_2$, protease inhibitor cocktail [PIC; 2 μg/ml antipain, 0.1% aprotinin, 10 μg/ml benzamidine, 1 μg/ml chymostatin, 1 μg/ml leupeptin, and 1 μg/ml pepstatin], pH 7.5) on ice for 1 h with trituration every 15 min. Insoluble material was pelleted by centrifugation (8,800 *g*; 5 min), and 100-μl aliquots were incubated with 50 μl (1.5 mg/ml) of either anti-GalTase IgG or normal rabbit IgG under constant rotation for 1 h at 4°C. Protein A–Sepharose was added as a 1:1 slurry in 100 μl of solubilization buffer, and the mixture was rotated for 0.5 h at 4°C. The Protein A–Sepharose IgG/GalTase complex was pelleted (8,800 *g*; 5 min), and 50 μl was assayed for GalTase activity towards *N*-acetylglucosamine using high voltage borate electrophoresis as described (34).

Surface GalTase Activity

^{125}I-Antibody Binding. Cultures of BALB/c 3T3 cells were (*a*) washed twice with medium B (127 mM NaCl, 5.3 mM KCl, 18.2 mM Na Hepes, pH 7.2) and incubated with 5% BSA, 0.02% NaN_3 at room temperature for 45 min; then (*b*) washed twice with medium B and incubated with 0.33 mg/ml of either anti-GalTase IgG or normal rabbit IgG in medium B, 0.5% BSA, 0.02% NaN_3 at room temperature for 45 min; and (*c*) washed twice in medium B, 2% BSA, 0.1% NaN_3 and incubated with 4.11 μCi ^{125}I-goat anti-rabbit IgG (DuPont Co., Wilmington, DE) in medium B, 0.5% BSA, 0.02% NaN_3 at room temperature for 45 min. Cells were washed twice with medium B, 2% BSA, 0.1% NaN_3 and solubilized with 1 N NaOH. The amount of solubilized radioactivity was determined in a minigamma counter (model 1275; LKB Instruments, Gaithersburg, MD). The concentrations of both the primary (i.e., rabbit IgG) and secondary (i.e., ^{125}I-goat IgG) antibodies were shown to be in excess.

Enzymatic Activity. BALB/c 3T3 cells were cultured and harvested as indicated above, washed once with complete media, and twice with medium B. For surface GalTase assays, cells were resuspended at 2.5×10^6 cells/ml medium B, PICs, 1% BSA. For total cellular GalTase activity, cells were resuspended at 0.8×10^6 cells/ml medium B, PICs containing 30 mM *n*-octylglucoside and solubilized on ice for 1 h. 40-μl aliquots were assayed for GalTase activity towards *N*-acetylglucosamine using high voltage borate electrophoresis. Background radioactivity (i.e., nonincubated controls) was subtracted from all assays incubated at 37°C.

Northern Blot Analysis

Sparse cultures of BALB/c 3T3 cells were cultured and harvested as described above. Total RNA was extracted as described (17) and denatured by heating at 60°C for 15 min in 50% (vol/vol) formamide, 6% (vol/vol) formaldehyde, 20 mM MOPS, 5 mM Na acetate, 1 mM EDTA. 10 μg RNA was electrophoresed on 1% agarose, 6% formaldehyde gels, transferred to nitrocellulose, and hybridized with the ^{32}P-labeled 5′ end 2.0-kb Eco RI fragment of a 3.1-kb murine GalTase cDNA isolated from an F9 embryonal carcinoma cell lambda gt10 library (17). Hybridization occurred overnight at 42°C in 5% dextran sulfate (wt/vol), 4× SSC (1× SSC = 0.15 M NaCl, 0.015 M Na citrate), 50% (vol/vol) formamide, 20 μg/ml salmon sperm DNA, 1× Denhart's solution, 50 mM Na phosphate (pH 7.0). After hybridization, the filters were washed once in 2× SSC, 1% SDS at room temperature, and twice in 0.5× SSC, 0.1% SDS at 45°C. The bands were visualized by autoradiography.

Indirect Immunofluorescence

Embryo mesenchymal cell explants were cultured in defined medium on either untreated or matrix-coated (laminin or fibronectin) glass chamber slides (Miles Scientific Div., Naperville, IL) and incubated for 2 d in 5% CO_2 at 37°C to allow cells to migrate from the explant. BALB/c 3T3 cells were cultured on matrix-coated coverslips. Cultures were washed three times with DME and incubated with DME, 2–5% BSA for 30 min at room temperature to block nonspecific adsorption. In some instances, cultures were prefixed in 10% formalin in medium B for 20 min before blocking with BSA. Cultures were washed twice with DME and subsequently incubated for 45–60 min in 100 μl of either 0.6 mg/ml anti-GalTase IgG or 0.6 mg/ml normal rabbit IgG in DME, 2% BSA. The cultures were washed twice with DME and incubated for 45–60 min at room temperature in 200 μl biotinylated goat anti-rabbit IgG (7.5 μg/ml in DME) (Vector Laboratories, Inc., Burlingame, CA). Cultures were again washed twice with DME and incubated for 45–60 min at room temperature in the dark with 200 μl Avidin DCS (20 μg/ml in DME) (Vector Laboratories, Inc.). After two additional washes in DME, cultures were either mounted as described below or permeabilized with 100 μl of −20°C acetone. 20 μl (1 U) of rhodamine-conjugated phalloidin (Molecular Probes Inc., Junction City, OR) was evaporated and resuspended in 150 μl of PBS, which was added to each well and incubated for 20 min at room temperature in the dark. Control incubations contained PBS rather than phalloidin. Slides were washed twice with PBS, mounted with medium (90% [vol/vol] glycerol, 10% [vol/vol] PBS, and 4% [wt/vol] *n*-propylgalate) and viewed with a microscope equipped for epifluorescence (Dialux EB 22; Leitz, Rockleigh, NJ).

Results

Experimental Rationale

Past studies suggest that GalTase is present on the surface of mesenchymal cells where it functions during cell migration by binding to its complementary substrate in the extracellular matrix (32, 34). Furthermore, perturbation of surface GalTase activity with competitive substrates and modifier proteins coincidentally perturbs the rate of avian neural crest cell migration on basal lamina (28). In the present study, we have taken advantage of an appropriate anti-GalTase IgG to (*a*) examine GalTase function during mouse mesenchymal cell migration; (*b*) quantitate the level of surface GalTase on migrating cells; and (*c*) define the plasma membrane distribution of GalTase by indirect immunofluorescence on cells migrating on various extracellular matrices. To approximate the in vivo situation as closely as possible, primary explants of embryonic mouse mesenchyme were used, but when quantitation was necessary BALB/c 3T3 mouse fibroblasts were used as an in vitro substitute. Appropriate controls showed that surface GalTase has a similar distribution on both cell types (see below).

Perturbing Surface GalTase Inhibits Cell Migration on Laminin-containing Matrices

The rate of mesenchymal cell migration was quantitated using a previously established in vitro assay (28). To control for variation in migration rates between individual cells within a population, as well as between cell populations from different explants, the basal migration rate for each population of cells was determined and compared to the migration rate for the same cell population in the presence of experimental reagents.

Two reagents were used that block GalTase binding to its glycoconjugate substrate: the substrate modifier protein, α-LA; and antisera raised against affinity-purified GalTase. α-LA binds to GalTase and modifies its substrate specificity away from its conventional substrate, *N*-acetylglucosamine, and towards glucose, a substrate of normally low affinity (18). The interaction between α-LA and GalTase is fairly specific, since GalTase can be purified to apparent homogeneity by α-LA affinity chromatography (16). Previous studies have shown that α-LA inhibits the migration rate of avian neural crest cells on laminin and laminin-containing matrices in a dose-dependent manner (28). As expected, α-LA (1.5 mg/ml) inhibited embryonic mouse mesenchymal cell migration ~50% as compared to basal rate. Lysozyme (1.5 mg/ml), a protein structurally similar to α-LA but without GalTase-modifying activity, did not affect cell migration (Table I).

Polyclonal rabbit anti-bovine milk GalTase IgG has been shown to specifically recognize GalTase in mouse cells by a variety of criteria (2, 16, 29, 30, 37). Similarly, anti-GalTase IgG can be shown to recognize embryonic mouse mesenchymal cell GalTase, since in this study it immunoprecipitated 90% of GalTase enzyme activity from detergent-solubilized mesenchymal cells as compared with control incubations containing normal rabbit IgG (normal rabbit IgG [1,517 ± 30 cpm product/50 μl/h] vs. anti-GalTase IgG [152 ± 3 cpm product/50 μl/h] remaining in the supernatant).

The rate of mesenchymal cell migration in the presence of anti-GalTase IgG is shown in Fig. 1. Cell migration during

Table I. α-LA Inhibits Mouse Mesenchyme Migration on Basal Lamina Substrates

Additions	Cell migration	Control
	μm/h	%
None (basal rate)	15.1 ± 2.5	100
α-LA	7.2 ± 1.2	48
None (basal rate)	13.5 ± 1.4	100
Lysozyme	15.1 ± 1.4	112

Mesenchymal cell migration on PYS basal lamina was quantitated by time-lapse microphotography as described in Materials and Methods. α-LA or lysozyme were added at 1.5 mg/ml. This experiment was repeated three times with similar results. α-LA inhibited cell migration similarly on purified laminin matrices. Data shown are ±SEM.

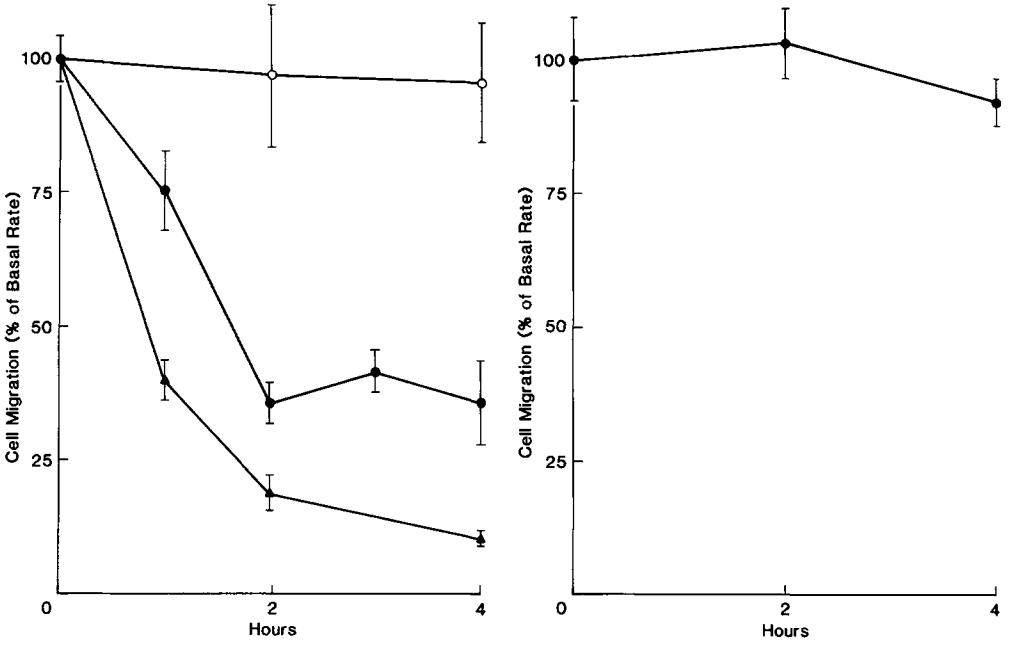

Figure 1. Anti-GalTase IgG inhibits cell migration on laminin-containing matrices. Each data point (±SEM) represents the average of two identical assays containing 0.23 mg/ml IgG. (*Left*) Cell migration on PYS-derived basal lamina. (*Right*) Cell migration on fibronectin. Similar results were found using purified laminin rather than PYS basal lamina. (●) Anti-GalTase IgG; (▲) anti-GalTase Fab fragments; (○) normal rabbit IgG.

the first hour of incubation was inhibited by ~25% and after 2 h reached 64% inhibition. The cumulative data from six experiments are shown in Table II. In all instances, anti-GalTase IgG inhibited cell migration compared with the basal rate, ranging from 48 to 80% inhibition (Table II). Anti-GalTase IgG produced variable effects on cell morphology, ranging from no noticeable morphological effects in some cultures to partly reducing cell spreading in others. These effects are analogous to the ability of anti-GalTase IgG to inhibit initial lamellipodial formation on laminin when added at the time of cell plating (29). Identical concentrations of preimmune or normal rabbit IgG had no significant effect on morphology or migration rate (Fig. 1; Table II).

To insure that anti-GalTase IgG was inhibiting cell migration by blocking GalTase sites rather than by nonspecific cross-linking effects, Fab fragments of anti-GalTase IgG were prepared and purified free of contaminating Fc fragments and intact IgG. The purified Fabs inhibited cell migration on laminin-containing matrices as shown in Fig. 1.

The specificity of anti-GalTase IgG inhibition was determined by assaying its effect on cells migrating on fibronectin.

Table II. Anti-GalTase IgG Inhibits Cell Migration on Basal Lamina Substrates

Additions	Cells/ explants	Migration	Basal rate	Range (of basal rate)
	n/n	*μm/h*	%	%
None (basal rate)	45/3	14.7 ± 1.8	(100)	
Normal rabbit IgG	45/3	14.9 ± 1.5	101	89–113
None (basal rate)	145/6	27.2 ± 2.1	(100)	
Anti-GalTase IgG	170/6	9.3 ± 1.4	34	20–52

The rate of cell migration on PYS basal lamina was quantitated as described in Materials and Methods. Migration rate after addition of 0.23 mg/ml normal rabbit IgG or 0.1–0.25 mg/ml anti-GalTase IgG was compared with basal rate. Rates shown represent the average migration rate during a 2-h period (2–4 h after IgG addition). Anti-GalTase IgG inhibited migration similarly on purified laminin matrices. Data shown are ±SEM.

Previous studies have shown that reagents that perturb surface GalTase inhibited migration on laminin matrices but did not affect migration on fibronectin substrates (28). As shown in Fig. 1, concentrations of anti-GalTase IgG that markedly inhibited cell migration on laminin matrices had no effect on migration rate on fibronectin. These results clearly eliminate nonspecific metabolic effects of anti-GalTase IgG and demonstrate strict substrate specificity for the involvement of GalTase during cell migration on laminin.

Surface GalTase Levels Are Elevated on Cells Migrating on Laminin

The expression of surface GalTase on cells cultured on various extracellular matrices was quantitated by ^{125}I-antibody binding and by direct enzyme assay. Since it was necessary to normalize GalTase levels to cell number, these studies relied upon cultured embryonic mouse fibroblasts (i.e., BALB/c 3T3 cells) rather than primary explants of embryonic mesenchyme in which cell number was highly variable. Furthermore, the use of 3T3 fibroblasts enabled comparisons of stationary cells in contact-inhibited, confluent cultures with migratory cells in sparse cultures.

Surface GalTase levels were similar on both stationary and migratory cells when cultured on either fibronectin-coated or plastic surfaces, as well as on stationary cells cultured on laminin (Table III). However, when cells migrated on laminin, surface GalTase was elevated threefold relative to all other culture conditions. Similar results were obtained using two independent assays for quantitating surface GalTase expression (i.e., ^{125}I-antibody binding and direct enzyme assay of intact cells).

In contrast to the levels of surface GalTase, total cellular GalTase activity was similar, per microgram of protein, in cells migrating on laminin or fibronectin (Fig. 2). The levels of GalTase mRNA were also relatively similar, per microgram of total RNA, in cells grown on laminin and fibronectin (Fig. 2). GalTase mRNA levels were slightly higher when

Table III. Laminin Increases Surface GalTase Expression on Sparse Cells

Assay	Cell phenotype	Substrate			Fold increase (laminin/fibronectin)
		Laminin	Fibronectin	Plastic	
Enzyme activity*	Stationary	295 ± 25	281 ± 15	310 ± 22	1.1
	Migratory	692 ± 13	288 ± 20	294 ± 17	2.4§
^{125}I-IgG binding‡	Migratory	19,962 ± 2,045	5,560 ± 520	ND	3.6§

BALB/c 3T3 fibroblasts were cultured on the indicated matrix as described in the Materials and Methods. Cells in >90% confluent cultures were considered to be stationary, while cells in sparse (<20% confluent) cultures were considered to be migratory.

* Enzyme activity toward *N*-acetylglucosamine substrates is expressed as pmol ^{3}H-galactose transferred per 10^6 cells/h ±SEM. Background radioactivity (nonincubated controls) was subtracted from all assays and averaged 236 cpm (equivalent to ~5 pmol).

‡ ^{125}I-IgG binding is expressed as specific cpm ^{125}I bound/10^4 cells ±SEM (i.e., normal rabbit IgG binding subtracted from anti-GalTase IgG binding). Normal rabbit IgG binding averaged 7,501 cpm/10^4 cells. There was no anti-GalTase IgG binding to matrices devoid of cells.

§ Values for laminin and fibronectin are significantly different from one another, $p < 0.005$.

cells were grown on uncoated plastic surfaces, suggesting that the cells were compensating for the lack of any extracellular matrix. In any event, laminin appears to increase the level of GalTase on the cell surface by recruiting enzyme from intracellular pools and not by increasing the level of total cell GalTase.

Laminin Induces GalTase Expression on Lamellipodia and Filopodia

The cell surface distribution of GalTase, as well as possible cytoskeletal associations, was determined on various extracellular matrices by double-label indirect immunofluorescence. When primary mesenchymal cell explants were grown on laminin matrices, GalTase was localized to the edge of cellular processes, such as lamellipodia and filopodia, as well as to areas of cell–cell contact (Fig. 3). There was no apparent uniform distribution of GalTase over the cell body; all immunoreactivity appeared to be localized to the leading and trailing edges of migrating cells. GalTase distribution was unaffected by including NaN_3 in all reagents or by prefixing in 10% formalin. We attempted to apply anti-GalTase IgG to the basal surface of the migratory cells by culturing cells on porous filters (12-mm Millicell CM; Millipore Continental Water Systems, Bedford, MA) and applying IgG from beneath the filter surface. However, very few cells adhered to and migrated on these filter surfaces, and those cells that were labeled showed a similar GalTase distribution to those that received antibody apically.

Fluorescently labeled cell "ghosts" were occasionally seen on laminin matrices, even though no cells were apparent using phase-contrast optics (Fig. 3, *e* and *f*). These fluorescent spikes appeared to radiate from the entire circumference of where a cell body had apparently been. We suspect that these reflect the membrane remnants of cells that had been dissociated from their laminin adhesion by anti-GalTase IgG, and are reminiscent of mesenchymal cell "retraction fibers" seen ultrastructurally (25). No such immunoreactivity was observed on laminin matrices that had not supported cell growth or when preimmune IgG was used.

Since we used cultured embryonic fibroblasts (i.e., BALB/c 3T3 cells) to quantitate surface GalTase expression on various extracellular matrices, we confirmed that the immunofluorescence distribution of surface GalTase was similar on cultured fibroblasts and on primary mesenchymal cells. Surface GalTase was localized to the leading and trailing edges of migrating 3T3 fibroblasts, similar to that seen on primary

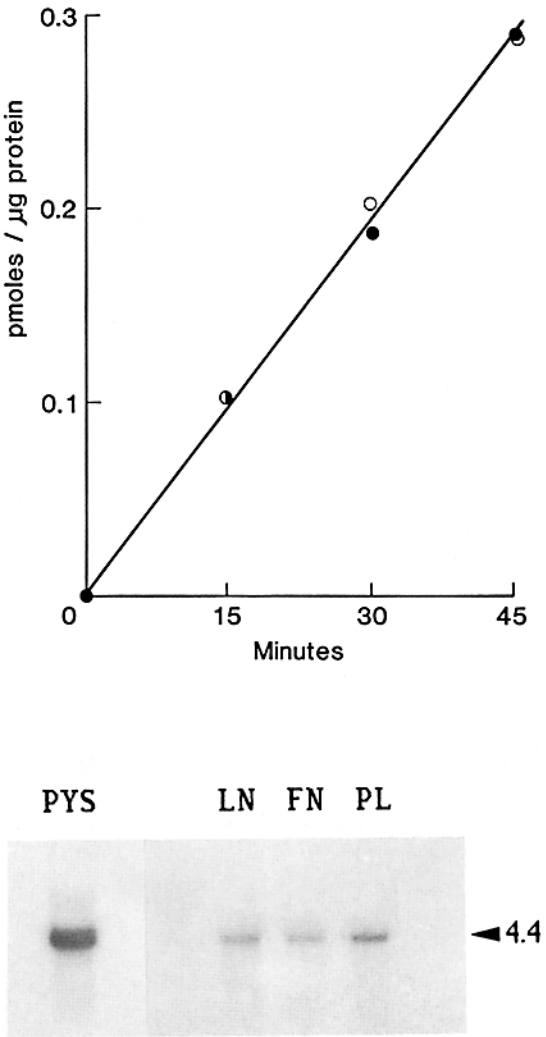

Figure 2. Total cellular GalTase is equal in cells cultured on laminin and on fibronectin. (*Top*) GalTase enzyme activity was assayed in total cell lysates as a function of incubation time as described in Materials and Methods. (○) Cells cultured on laminin; (●) cells cultured on fibronectin. (*Bottom*) GalTase mRNA levels were determined by Northern blot analysis as described in Materials and Methods. The GalTase cDNA hybridizes with a 4.4-kb mRNA species. PYS cells, which have high levels of GalTase mRNA, were used as a positive control (17). *LN*, cells cultured on laminin; *FN*, cells cultured on fibronectin; *PL*, cells cultured on tissue culture plastic.

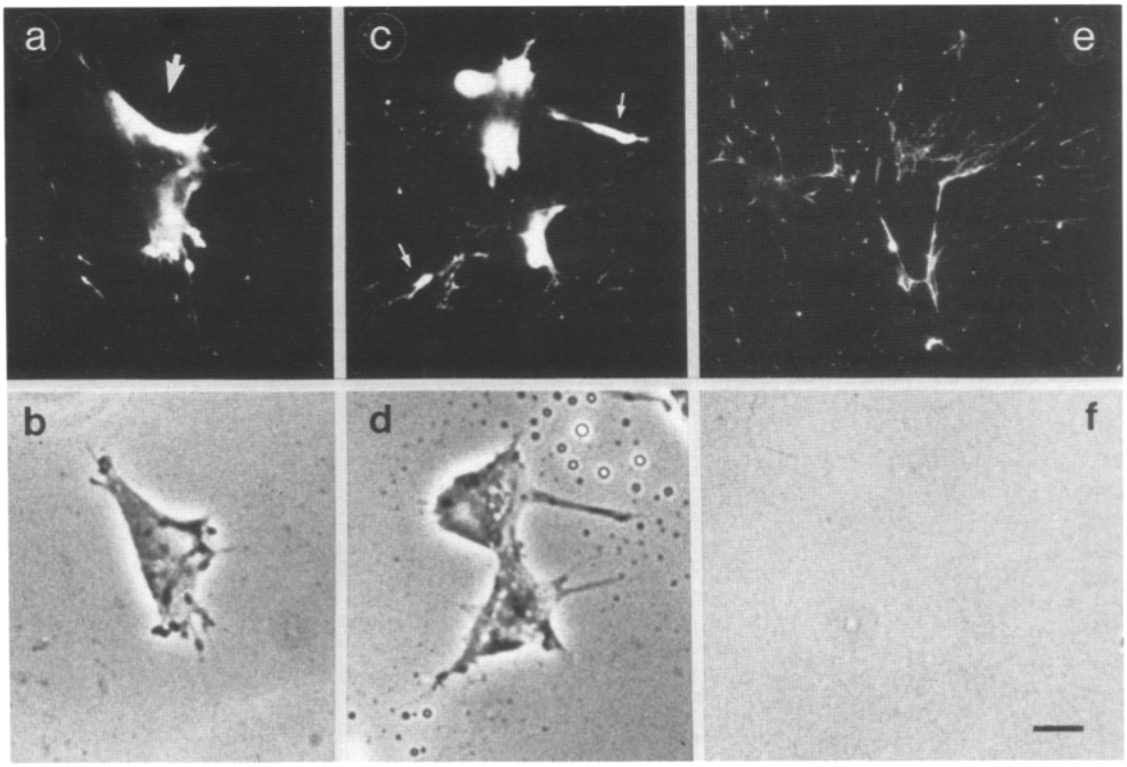

Figure 3. Surface GalTase is localized by indirect immunofluorescence to the leading and trailing edges of embryonic mesenchymal cells migrating on laminin. Examples of GalTase localization to lamellipodia (*large arrow*) and filopodia (*small arrows*) are shown on lightly formalin-fixed cells. Some areas have no cell structures as shown by phase-contrast optics (*f*) but showed cell outlines or "ghosts" by indirect immunofluorescence (*e*). There was no cytoskeletal staining seen in association with the cell "ghosts" (data not shown). (*a*, *c*, and *e*) Anti-GalTase IgG immunofluorescence; (*b*, *d*, and *f*) phase-contrast image. Bar, 10 μm.

mesenchymal cell explants, although the label appeared more punctate on cultured 3T3 fibroblasts (Fig. 4). Sparse cultures of 3T3 fibroblasts contain cells in various stages of migration, ranging from stationary fibroblastic cells to polarized migrating cells with broad lamellipodia; therefore, it is possible to reconstruct the polarization of GalTase from a uniform distribution on stationary, fibroblastic cells (Fig. 4 *a*) to broad lamellipodia characteristic of migratory cells (Fig. 4 *e*). The microspike distribution of surface GalTase was particularly evident on stationary cells (Fig. 4 *a*), which

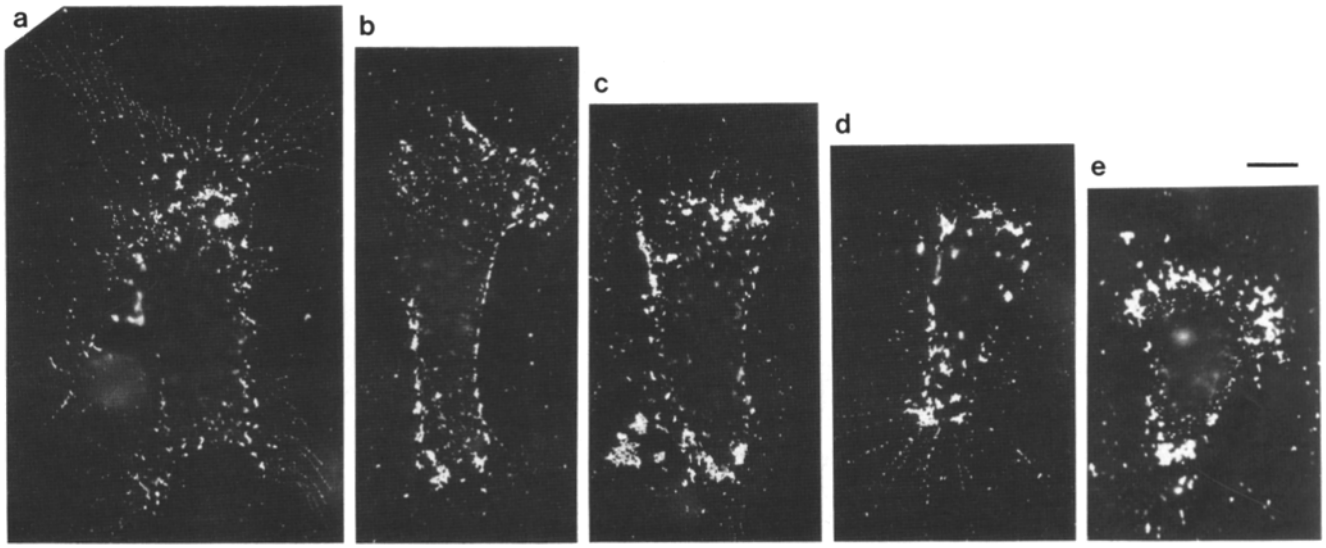

Figure 4. Surface GalTase becomes polarized to lamellipodia on migrating mouse fibroblasts cultured on laminin. Examples of GalTase immunofluorescence distribution on unfixed BALB/c 3T3 fibroblasts showing progressive stages of polarization from stationary to migratory cells. Bar, 10 μm.

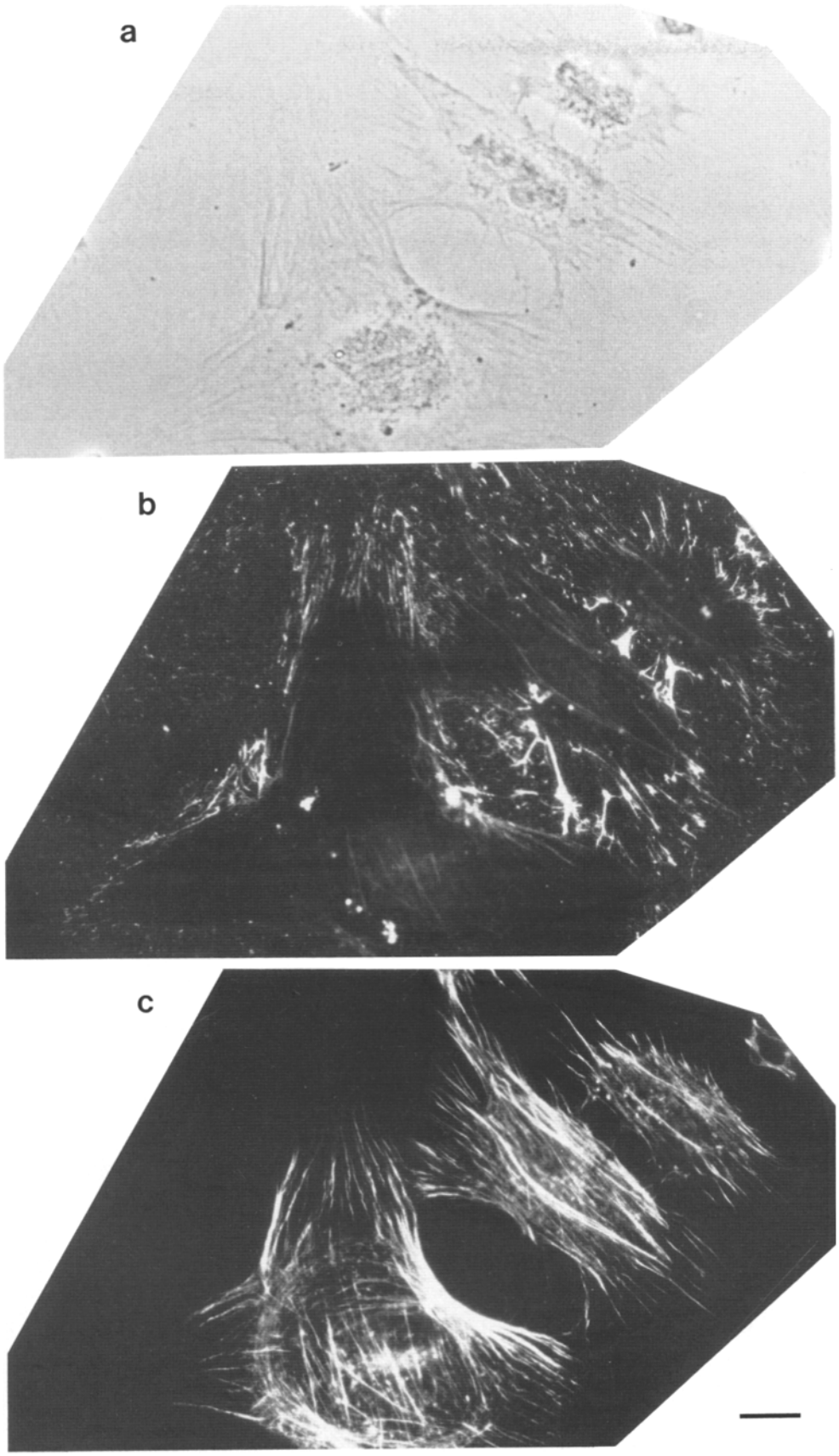

Figure 5. The distribution of surface GalTase colocalizes with some actin microfilaments in embryonic mesenchymal cells cultured on laminin. Acetone permeabilization removed most of the lamellipodial staining seen in Fig. 3, but some filopodia still stain with both anti-GalTase IgG and phalloidin. Some GalTase is localized on fine filopodia between cells devoid of microfilaments. (*a*) Phase-contrast image; (*b*) anti-GalTase IgG immunofluorescence; (*c*) rhodamine-labeled phalloidin indicates the distribution of filamentous actin. Bar, 10 μm.

appeared to retract as cells assumed a more migratory appearance. Since virtually all cells in primary mesenchymal cell explants were actively migrating, they all displayed surface GalTase similar to that seen on migrating 3T3 fibroblasts (compare Fig. 3, *a* and *c*, with Fig. 4 *e*). None of the cells in primary explants displayed surface GalTase indicative of stationary cells as seen in Fig. 4 *a*.

The distribution of microfilaments was visualized using rhodamine-labeled phalloidin in acetone-permeabilized cells in primary mesenchymal cell explants (Fig. 5). Acetone permeabilization removed all broad lamellipodial staining produced by anti-GalTase IgG. However, filopodial staining was resistant to acetone treatment, and in these areas there was an apparent colocalization of surface GalTase with filamentous actin, although some GalTase was localized on fine filopodia devoid of microfilaments.

When cells were grown on fibronectin substrates, surface GalTase was not detectable on cell lamellipodia or filopodia (Fig. 6). Similar results were obtained using either primary mesenchymal cell explants (Fig. 6) or sparse cultures of BALB/c 3T3 fibroblasts (not shown). These results suggest that the threefold increase in surface GalTase seen on laminin matrices was due to a specific expression of GalTase onto lamellipodia and filopodia. In all instances, normal rabbit IgG produced background levels of fluorescence (Fig. 7).

Discussion

The function, distribution, and relative expression of surface GalTase during cell migration on various extracellular matrices has been examined. Anti-GalTase IgG specifically recognizes murine GalTase by a variety of criteria (2, 16, 29, 30, 37) and inhibited cell migration on laminin substrates but not on fibronectin substrates. The effects of the GalTase modifier protein, α-LA, are consistent with these findings. Furthermore, the level of surface GalTase was elevated threefold when cells migrated on laminin, relative to cells migrating on either fibronectin or plastic surfaces, or relative to stationary, contact-inhibited cells on any surface. The laminin-dependent increase in surface GalTase was due to the stable expression of GalTase selectively on lamellipodia and filopodia at the leading and trailing edges of migrating cells. GalTase was localized in specific plasma membrane domains by recruitment from intracellular pools rather than clustering of uniformly distributed surface GalTase, as shown recently for the fibronectin receptor (3, 5, 6, 38). GalTase was not detectable on lamellipodia or filopodia when cells migrated on fibronectin, consistent with the fact that fibronectin-mediated cell migration is independent of surface GalTase. On all substrates examined, the amount of total cellular GalTase remained relatively constant as judged by enzyme activity and Northern blot analysis.

These results support the notion that surface GalTase functions during cell migration on basal lamina matrices (28, 29). Collectively, results in this and previous studies show that three different classes of reagents, including anti-GalTase IgG, the modifier protein α-LA, and competitive *N*-acetylglucosamine substrates, all of which inhibit GalTase binding to its complementary glycoconjugate substrate, coincidently inhibit the rate of cell migration on basal lamina, but not on fibronectin. Conversely the addition of UDPgalactose, which increases the catalytic turnover of the GalTase–substrate complex, increases the rate of cell migration on basal lamina. In all instances, homologous control reagents

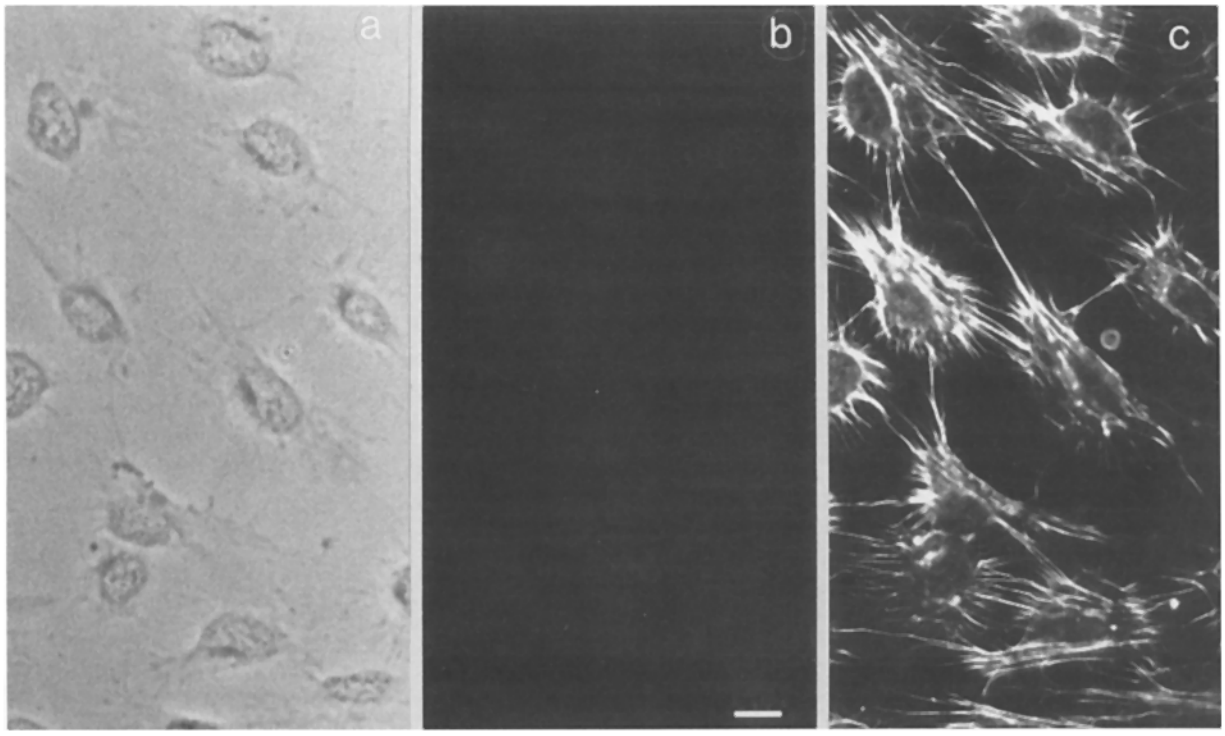

Figure 6. No surface GalTase is detectable on embryonic mesenchymal cells migrating on fibronectin. (*a*) Phase-contrast image; (*b*) anti-GalTase IgG immunofluorescence; (*c*) phalloidin staining of filamentous actin. Bar, 10 μm.

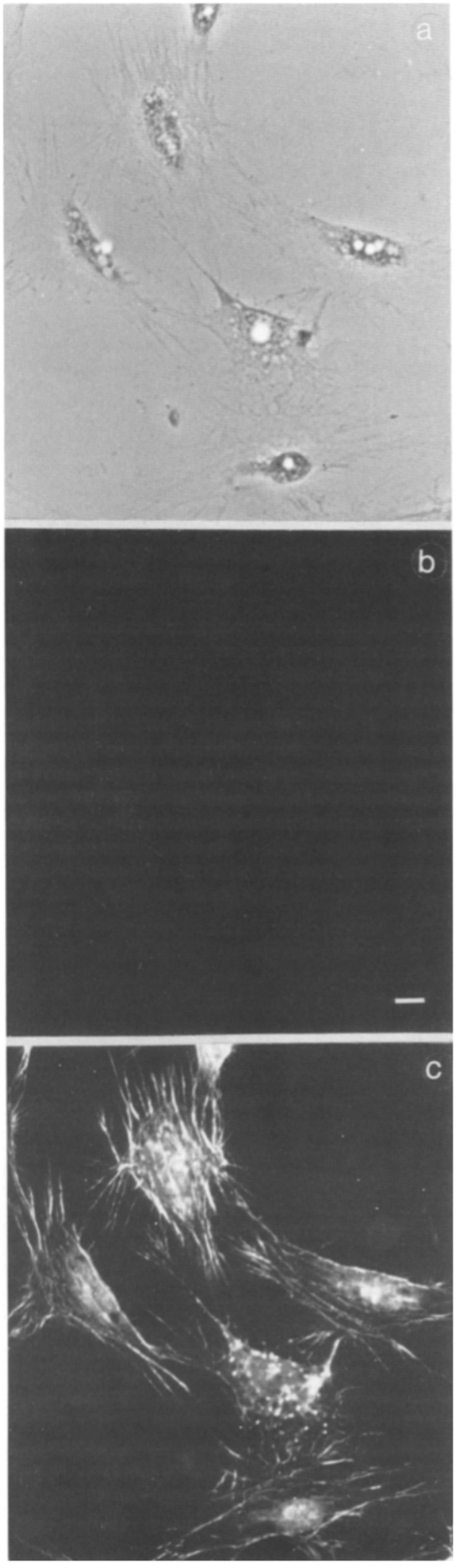

have no effect on surface GalTase activity or on cell migration rate.

One of the more surprising findings in this study was the selective ability of laminin matrices, relative to fibronectin, to induce GalTase expression onto lamellipodia and filopodia. This was confirmed by quantitating the level of surface GalTase by ^{125}I-antibody binding and by direct enzyme assay of intact cells. There is increasing evidence that the extracellular matrix, and basal lamina in particular, induces cell type–specific protein expression (15); however, in this study, GalTase mRNA levels were relatively unaffected by laminin within the 24-h culture period. The slight (i.e., 33%) increase in GalTase mRNA levels in cells cultured on laminin may represent the initial stages of laminin induction of GalTase mRNA, but this must be analyzed after longer culture periods. In any event, the levels of total cellular GalTase activity were unaffected by laminin and, therefore, this implies that laminin induced the recruitment of GalTase from intracellular pools to the growing lamellipodia. These results also show that the level of surface GalTase does not simply reflect the level of intracellular GalTase and, therefore, the surface and intracellular pools of GalTase must be differentially regulated. The expression of GalTase on the cell surface does not result from passive movement of Golgi region–derived vesicles to the plasma membrane, since lamellipodia developing on fibronectin matrices would be expected to contain GalTase as well. Since laminin contains substrates for surface GalTase, while fibronectin does not, it should also be considered that surface GalTase expression is stabilized by binding extracellular substrates.

The function of GalTase can be distinguished from that of other previously identified laminin receptors (7, 13, 22) biologically and biochemically. A number of laminin-binding proteins bind to laminin affinity columns, including the 68-kD receptor and GalTase, but they are differentially eluted (29). Reagents that inhibit GalTase binding to its laminin substrate also inhibit cell spreading and migration on laminin, but do not affect initial cell adhesion to laminin (29). On the other hand, consuming potential GalTase binding sites in laminin by prior galactosylation does not inhibit cell adhesion to laminin, but totally inhibits cell spreading and migration (29). These results suggest that initial adhesion to laminin may be mediated by the binding of the 68-kD and/or 140-kD (i.e., integrin) receptor to their peptide ligands (9), while cell spreading and subsequent migration requires surface GalTase binding to its appropriate N-linked oligosaccharide substrate. We are presently characterizing the binding sites within laminin for surface GalTase to determine their relationship to laminin fragments (e.g., E1, E8) that have differential effects on cell adhesion and migration (1, 8).

The potential association of GalTase with cytoskeletal components was assayed by double-labeled indirect immunofluorescence and phalloidin staining. Actin-containing microfilaments terminating in lamellipodia appeared to coincide with GalTase immunoreactivity, though some GalTase was localized on cell surface projections devoid of microfila-

Figure 7. Embryonic mesenchymal cells cultured on laminin and incubated with normal rabbit IgG show no detectable fluorescence. (*a*) Phase-contrast image; (*b*) immunofluorescence; (*c*) rhodamine-phalloidin staining of filamentous actin. Bar, 10 μm.

ments. It has recently been reported that the redistribution of surface GalTase that occurs during spermatogenic differentiation coincides with the appearance of actin-containing microfilaments (30), and patches of surface GalTase on Madin–Darby bovine kidney cells colocalize with actin microfilaments (31). Both results suggest an association between surface GalTase and cytoskeletal components. More detailed ultrastructural and biochemical studies are required to define the relationship between the cytoskeleton and GalTase, as has been done extensively for the fibronectin receptor (11).

While different cell surface receptors seem to function during cell migration on different extracellular matrices, all receptor–matrix interactions must provide a mechanism for dissociation from the matrix to continue cell migration. How cells dissociate from the matrix is presently unknown, but it is interesting that GalTase offers a potential catalytic mechanism whereby cell adhesion to the substrate could be released if a suitable galactose donor were available to the surface enzyme. The galactose donor would then enable the enzyme to dissociate from its galactosylated substrate. In this regard, Turley and Roth (40) have shown that cells spontaneously glycosylate extracellular matrices coincident with migration upon them. Alternatively, it is possible that dissociation is due to shedding or proteolytic release of the surface receptor from the membrane. In this study, GalTase was detectable on microspikes surrounding cell "ghosts," suggesting that the enzyme, and possibly associated membrane, have been left behind after cell dissociation (23). In either case, it is clear that GalTase functions as a receptor during cell migration on basal lamina, presumably by interacting with specific N-linked oligosaccharide residues in laminin. Further studies are needed to define the mechanism of cell dissociation from the matrix, the cytoskeletal association with GalTase at the ultrastructural level, and how laminin induces the vectoral insertion of GalTase into growing lamellipodia.

The authors are grateful to Ms. Carol Neely for the initial preparation of anti-GalTase IgG, to Dr. Paul Begovac for preparation of the Fab fragments, and to Ms. Ellen Madson and Mrs. San Juanita De La Cerda for preparing the manuscript.

This study was supported by grant DE 07120 from the National Institutes of Health to B. D. Shur, and by a Rosalie B. Hite predoctoral fellowship to D. J. Eckstein.

Received for publication 3 January 1989 and in revised form 13 February 1989.

References

1. Aumailley, M., V. Nurcombe, D. Edgars, M. Paulson, and R. Timpl. 1987. The cellular interactions of laminin fragments. *J. Biol. Chem.* 262:11532–11538.
2. Bayna, E. M., J. H. Shaper, and B. D. Shur. 1988. Temporally-specific involvement of cell surface galactosyltransferase during mouse embryo morula compaction. *Cell.* 53:145–157.
3. Brown, P. J., and R. L. Juliano. 1987. Association between fibronectin receptor and the substratum: spare receptors for cell adhesion. *Exp. Cell Res.* 171:376–388.
4. Charonis, A. S., A. P. N. Skubitz, G. G. Koliakos, L. A. Reger, J. Dege, A. M. Vogel, R. Wohlhueter, and L. T. Furcht. 1988. A novel synthetic peptide from the B1 chain of laminin with heparin-binding and cell adhesion-promoting activities. *J. Cell Biol.* 107:1253–1260.
5. Dejana, E., S. Colella, G. Conforti, M. Abbadini, M. Gaboli, and P. C. Marchisio. 1988. Fibronectin and vitronectin regulate the organization of their respective Arg-Gly-Asp adhesion receptors in cultured human endothelial cells. *J. Cell Biol.* 107:1215–1223.
6. Duband, J.-L., G. H. Nuckolls, A. Ishihara, T. Hasegawa, K. M. Yamada, J. P. Thiery, and K. Jacobson. 1988. Fibronectin receptor exhibits high lateral mobility in embryonic locomoting cells but is immobile in focal contacts and fibrillar streaks in stationary cells. *J. Cell Biol.* 107:1385–1396.
7. Gehlsen, K. R., L. Dillner, E. Engvall, and E. Ruoslahti. 1988. The human laminin receptor is a member of the integrin family of cell adhesion receptors. *Science (Wash. DC).* 241:1228–1229.
8. Goodman, S. L., R. Deutzmann, and K. Von der Mark. 1987. Two distinct cell binding domains in laminin can independently promote nonneuronal cell adhesion and spreading. *J. Cell Biol.* 105:589–598.
9. Graf, J., Y. Iwamoto, M. Sasaki, G. R. Martin, H. K. Kleinman, F. A. Robey, and Y. Yamada. 1987. Identification of an amino acid sequence in laminin mediating cell attachment, chemotaxis, and receptor binding. *Cell.* 48:989–996.
10. Hall, D. E., K. A. Frazer, B. C. Hann, and L. F. Reichardt. 1988. Isolation and characterization of a laminin-binding protein from rat and chick muscle. *J. Cell Biol.* 107:687–697.
11. Horwitz, A., K. Duggan, C. Buck, M. C. Beckerle, and K. Burridge. 1986. Interaction of plasma membrane fibronectin receptor with talin: a transmembrane linkage. *Nature (Lond.).* 320:531–533.
12. Humphreys-Beher, M. G., C. A. Schneyer, V. S. Kidd, and R. B. Marchase. 1987. Isoproterenol-mediated parotid gland hypertrophy is inhibited by effectors of 4β galactosyltransferase. *J. Biol. Chem.* 262: 11706–11713.
13. Kleinman, H. K., R. C. Ogle, F. B. Cannon, C. D. Little, T. M. Sweeney, and L. Luckenbill-Edds. 1988. Laminin receptors for neurite formation. *Proc. Natl. Acad. Sci. USA.* 85:1282–1286.
14. LeDouarin, N. M. 1984. Cell migration in embryos. *Cell.* 38:353–360.
15. Li, M. L., J. Aggeler, D. A. Farson, C. Hatier, J. Hassell, and M. J. Bissell. 1987. Influence of a reconstituted basement membrane and its components on casein gene expression and secretion in mouse mammary epithelial cells. *Proc. Natl. Acad. Sci. USA.* 84:136–140.
16. Lopez, L. C., E. Bayna, D. Litoff, N. Shaper, J. Shaper, and B. D. Shur. 1985. The receptor function of mouse sperm surface galactosyltransferase during fertilization. *J. Cell Biol.* 101:1501–1510.
17. Lopez, L. C., C. M. Maillet, K. Oleszkowicz, and B. D. Shur. 1989. Cell surface and Golgi pools of β1,4 galactosyltransferase are differentially regulated during embryonal carcinoma cell differentiation. *Mol. Cell. Biol.* In press.
18. Morrison, J. F., and K. E. Ebner. 1971. Studies on galactosyltransferase: kinetic effects of alpha-lactalbumin with *N*-acetylglucosamine and glucose as galactosyltransferase group acceptors. *J. Biol. Chem.* 246:3992–3998.
19. Newgreen, D. F. 1984. Spreading of explants of embryonic chick mesenchymes and epithelia on fibronectin and laminin. *Cell Tissue Res.* 236: 265–277.
20. Perris, R., Y. von Boxberg, and J. Lofberg. 1988. Local embryonic matrices determine region-specific phenotypes in neural crest cells. *Science (Wash. DC).* 241:86–89.
21. Pintar, J. E. 1978. Distribution and synthesis of glycosaminoglycans during quail neural crest morphogenesis. *Dev. Biol.* 67:444–464.
22. Rao, N. C., S. H. Barsky, V. P. Terranova, and L. A. Liotta. 1983. Isolation of a tumor cell laminin receptor. *Biochem. Biophys. Res. Commun.* 111:804–808.
23. Revel, J.-P., and M. Solursh. 1978. Ultrastructure of primary mesenchyme in chick and rat embryos. *Scanning Electron Microsc.* II:1041–1046.
24. Roth, S. 1973. A molecular model for cell interactions. *Quart. Rev. Biol.* 48:541–563.
25. Roth, S., and D. White. 1972. Intercellular contact and cell-surface galactosyltransferase activity. *Proc. Natl. Acad. Sci. USA.* 69:485–489.
26. Rouslahti, E., and M. D. Piersbacher. 1987. New perspectives in cell adhesion: RGD and integrins. *Science (Wash. DC).* 238:491–497.
27. Rovasio, R. A., A. DeLouvee, K. M. Yamada, R. Timpl, and J.-P. Thiery. 1983. Neural crest cell migration: requirements for exogenous fibronectin and high cell density. *J. Cell Biol.* 96:462–473.
28. Runyan, R. B., G. D. Maxwell, and B. D. Shur. 1986. Evidence for a novel enzymatic mechanism of neural crest cell migration on extracellular glycoconjugate matrices. *J. Cell Biol.* 102:432–441.
29. Runyan, R. B., J. Versalovic, and B. D. Shur. 1988. Functionally distinct laminin receptors mediate cell adhesion and spreading: the requirement for surface galactosyltransferase in cell spreading. *J. Cell Biol.* 107: 1863–1871.
30. Scully, N. F., J. Shaper, and B. D. Shur. 1987. Spatial and temporal expression of cell surface galactosyltransferase during mouse spermatogenesis and epididymal maturation. *Dev. Biol.* 124:111–124.
31. Shaper, N. L., P. L. Mann, and J. H. Shaper. 1985. Cell surface galactosyltransferase: immunochemical localization. *J. Cell. Biochem.* 28: 229–239.
32. Shur, B. D. 1977. Cell surface glycosyltransferases in gastrulating chick embryos. I. Temporally and spatially specific patterns of four endogenous glycosyltransferase activities. *Dev. Biol.* 58:33–39.
33. Shur, B. D. 1977. Cell surface glycosyltransferases in gastrulating chick embryos. II. Biochemical evidence for a surface localization of endogenous glycosyltransferase activities. *Dev. Biol.* 58:40–55.
34. Shur, B. D. 1982. Cell surface galactosyltransferase activities during nor-

mal and mutant (*T/T*) mesenchyme migration. *Dev. Biol.* 91:149–162.
35. Shur, B. D. 1983. Embryonal carcinoma cell adhesion: the role of surface galactosyltransferase and its 90K lactosaminoglycan substrate. *Dev. Biol.* 99:360–372.
36. Shur, B. D., and D. Bennett. 1979. A specific defect in galactosyltransferase regulation on sperm bearing mutant alleles of the *T/t* locus. *Dev. Biol.* 71:243–259.
37. Shur, B. D., and C. A. Neely. 1988. Plasma membrane association, purification, and partial characterization of mouse sperm β1,4 galactosyltransferase. *J. Biol. Chem.* 263:17706–17714.
38. Singer, I. I., S. Scott, D. W. Kawka, D. M. Kazazis, J. Gailit, and E. Ruoslahti. 1988. Cell surface distribution of fibronectin and vitronectin receptors depends on substrate composition and extracellular matrix accumulation. *J. Cell Biol.* 106:2171–2182.
39. Tomaselli, K. J., C. H. Damsky, and L. F. Reichardt. 1988. Purification and characterization of mammalian integrin expressed by a rat neuronal cell line (PC12): evidence that they function as α/β heterodimeric receptors for laminin and type IV collagen. *J. Cell Biol.* 107:1241–1252.
40. Turley, E. A., and S. Roth. 1979. Spontaneous glycosylation of glycosaminoglycan substrates by adherent fibroblasts. *Cell.* 17:109–115.
41. Von der Mark, K., and U. Kuhl. 1985. Laminin and its receptor. *Biochim. Biophys. Acta.* 823:147–160.